FLOW CHARACTERISTICS OF A TWO-DIMENSIONAL NEUTRALLY BUOYANT JET IN A MODEL SETTLING TANK

Younghan Kim[1], Il Won Seo[2], and Jungkyu Ahn[3]

[1]Grad. Student, Department of Civil Engineering, Seoul National University, Seoul, Korea
[2]Assoc. Prof., Department of Civil Engineering, Seoul National University, Seoul, Korea
[3]Grad. Student, Department of Civil Engineering, Seoul National University, Seoul, Korea

Abstract: In this study, laboratory experiments were performed to investigate the flow characteristics of a two-dimensional neutrally buoyant jet in the inlet region of a rectangular laboratory settling tank. Velocity measurements were made with a three-component ADV. Two types of baffles were installed in front of a two-dimensional slot; a one-sided and a two-sided baffle. The flow fields from a plane jet impinging on these two types of baffles and a plane jet without a baffle showed quite different characteristics. To concentrate on investigating these flow characteristics, the effects of density currents due to temperature difference or the presence of sediments were not studied. Results of the experiments reveal that the use of the two-sided baffle results in the shortest inlet region. Also shown is that, in addition to the types of baffles, the Froude number turns out to be an important factor in the extent of the inlet region.

Key Words: settling tank, two-dimensional jet, recirculation, baffle, laboratory experiment

1. INTRODUCTION

In a settling tank, it is necessary to separate particulate solids from the clear water. This separation is traditionally achieved by gravitational sedimentation in a settling tank. Because this phase occupies a large portion of the operational cost of water treatment plants, it is very important to improve the solid removal efficiency. Because efficiency is in turn influenced significantly by hydrodynamic characteristics, it is essential to study these hydraulic processes by either numerical or hydraulic modeling.

An idealized assumption to describe the flow and sedimentation processes in rectangular settling tanks was introduced by Hazen (1904). The overflow rate concept, which is still the basis of most of today's design processes of the settling tank, is derived directly from Hazen's approach. Of course the assumption of the basic plug-flow (uniform horizontal velocity field) is a crude simplification of very complex flows encountered in practice, which has been known since the prototype measurements of velocities and suspended solids concentrations in a center-fed circular secondary settling tank by Anderson (1945). Although there have been significant numerical and experimental developments, the

design of the settling tank depends largely on empirical approaches with correcting factors introduced. A common technique treating the settling tank essentially as a black box is using the flow-through curves (FTC) to evaluate the hydraulic efficiency. However, a better understanding of the detailed hydraulic processes in the settling is crucial because of the strong interaction of the flow and sediments.

Relatively very few experiments have been performed compared to the numerical analysis mainly due to the difficulty of measurements of the turbulent velocity. Since Lyn and Rodi (1989) measured turbulence characteristics for neutrally buoyant inlet flow in a settling tank, there have been several experimental studies on density current effects in settling tanks. Krebs et al. (1995) performed density current experiments under various conditions of depths and discharges and showed that density currents stabilize the flow and that the overflow rate concept can no longer be applicable in these circumstances. Krebs et.al. (1998) carried out experiments on buoyancy-influenced flow, and Raju et al. (1999) studied sedimentation removal efficiency with and without flushing and proposed a removal efficiency formula.

In this study, measurements of turbulent characteristics induced by a two-dimensional neutrally buoyant jet were performed. Flow characteristics with various types of baffles were investigated in the experiments of the settling tank.

2. EXPERIMENTS

2. 1 Experimental Setup

The experimental model tank has the dimensions of length L=12 m, width B=1.53 m, and the channel depth is 1.0 m deep as shown in Fig. 1. The working area as a settling tank is about 6 m long. The inlet is a two-dimensional slot whose opening (h_i) is 2 cm wide. This inlet is made of Plexiglas and extends across the entire channel width in order to ensure two-dimensionality. The center of the opening is located 19 cm from the bottom. A free overflow over an inclined tailgate at the downstream end provides the outlet flow.

Velocity measurements were taken in the flows with two different types of baffles and without any baffle. The configurations of both type baffles are shown schematically in Figs. 2 (a) and (b). While the one-sided baffle extended all the way above the free surface and therefore forced flow to be deflected only under the baffle, the two-sided baffle allowed the flow to go above and below the baffle. These baffles are made of 2 cm thick Plexiglas.

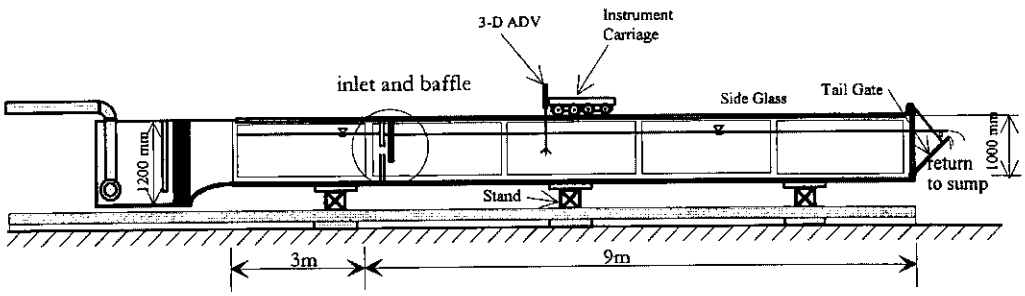

Fig. 1. Experimental Tank (side view)

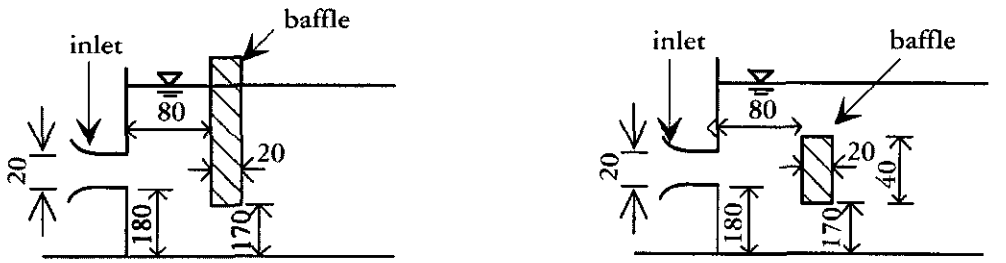

(a) One-sided Baffle (side view)

(b) Two-sided Baffle (side view)

Fig. 2. Experimental tank and details of baffles (unit : mm)

An electromagnctic flowmeter was used to measure the total discharge, Q. Velocity measurements were done by a three-component Acoustic Doppler Velocimeter(ADV). The velocity data, sampled at 25 Hz by the ADV, was collected by a data logger and stored in a hard disk of a laboratory PC. The sensor of the ADV was mounted on an automatic traverse system and controlled by a computer so as to be positioned at the desired points with the accuracy of 0.1 mm. Velocity profiles were acquired by measuring velocity components with 1 cm spacing vertically. However, the vertical spacing was reduced to 0.5 cm where finer resolution is required, for example, where a shear layer is expected. Unfortunately, it was not possible to get the velocity measurements near the free surface and the channel bottom because of the limitations of the ADV and the carriage. Using the ADV, velocities at each point were measured for 30 seconds. Thus, a total number of 750 velocity data were collected for each point in order to obtain the mean velocity and the turbulent characteristics.

2.2 Similitude Laws

Even though this study doesn't model any particular prototype tank, the condition in the model tank was required to represent a reasonable operation range with regard to a real one. The Froude number ($F = U / \sqrt{gH}$), where U is nominal average velocity, and H is water depth, is generally considered important in free surface flows and the Froude law is followed in most hydraulic modeling problems, but since the typical F in prototype settling tanks is very small, e.g., $O(10^{-6})$, it is almost impossible to maintain the model F that low while still maintaining the flow turbulent. Thus, following Lyn and Rodi (1989), it is taken that strict adherence to Froude-number similarity is unnecessary in settling tank modeling, provided F<<1. Of course a sufficiently high Reynolds number, $R=UH/\square$ (or $R_r=4R_HU/\square$, based on the hydraulic radius, R_H), where v is the kinematic viscosity of water, is required to insure that the flow remains turbulent. The criterion $R_r = 2000$ for turbulent flow, generally accepted in pipe flow, is adopted in this experiment. In prototype settling tanks, the Reynolds numbers are around 10,000. In the absence of density difference and sediments, two other numbers, the densimetric Froude number (the ratio of buoyancy and inertia forces) and the Hazen number (the ratio of flow velocities and settling velocities), are not relevant to this study

Table 1. Experimental Conditions

Case	Q (*l/sec*)	H (*cm*)	U (*cm/sec*)	U_i (*cm/sec*)	**R**	**F**	Baffle
I	8.33	40.0	1.36	27.23	5446	0.0069	None
II	8.33	40.0	1.36	27.23	5446	0.0069	One-sided
III	8.33	40.0	1.36	27.23	5446	0.0069	Two-sided
IV	8.33	30.0	1.82	27.23	5446	0.0106	None
V	8.33	30.0	1.82	27.23	5446	0.0141	Two-sided
VI	11.11	30.0	2.42	36.31	7262	0.0141	None
VII	11.11	30.0	1.82	36.31	7262	0.0141	Two-sided
VIII	11.11	40.0	1.82	36.31	7262	0.0092	None
IX	11.11	40.0	1.82	36.31	7262	0.0092	Two-sided

2.3 Experimental Conditions

The experiments performed in this study are classified into several cases shown in Table 1. The center of the inlet opening is fixed at 19 cm from the bottom for all experiments. The discharges were selected such that the Reynolds numbers were high enough ($\mathbf{R}_r$>2,000, **R**>2,000 more conservatively) to ensure turbulent flows, and the Froude numbers were kept low, but not as low as the prototype **F**, in order for the velocity measurements to be done with reasonable accuracy. In the table, U_i stands for nominal inlet velocity, $Q/(Bh_i)$, where Q is the total flow rate, B is the width of the flume, and h_i is the opening of the inlet.

3. ANALYSIS OF EXPERIMENTAL RESULTS

In all six experimental cases, centerline vertical velocity profiles were taken at a location along the channel, i.e., 4 cm, 13 cm, 50 cm, 100 cm, 150 cm, 200 cm, 300 cm, 400 cm, and 500 cm from the inlet. In the remaining three experiments where recirculation ends in a shorter distance, a few measurement points far downstream were omitted. The first measurement point (x = 4 cm : distance from the inlet) is midway between the inlet and the baffle, which is the nearest point to the inlet measurable by the ADV, and the next point (x = 13 cm) is the nearest measurable point at the downstream side of the baffle.

Fig. 3 shows flow characteristics near the inlet for Cases I, II, and III (Q=8.33 l/sec, H=40 cm). In this figure, $\bar{u}$ and $\bar{w}$ are the mean velocities in the longitudinal and vertical directions, which are defined as

$$\bar{u} = \frac{1}{T}\int_0^T u\,dt \tag{1}$$

$$\bar{w} = \frac{1}{T}\int_0^T w\,dt \tag{2}$$

where T = averaging interval, u = instantaneous velocity in the longitudinal direction, and w = instantaneous velocity in the vertical direction. $-\overline{u'w'}$ is the Reynolds shear stress which is defined as

$$-\overline{u'w'} = -\frac{1}{T}\int_0^T u'w'\,dt \tag{3}$$

where u' and w' are velocity fluctuations

given as

$$u' = u - \bar{u} \tag{4}$$

$$w' = w - \bar{w}. \tag{5}$$

The turbulent kinetic energy, k, is the quantity defined as

$$k = 0.75(\overline{u'^2} + \overline{w'^2}) \tag{6}$$

where

$$\overline{u'^2} = \frac{1}{T}\int_0^T u'^2\, dt \tag{7}$$

$$\overline{w'^2} = \frac{1}{T}\int_0^T w'^2\, dt \tag{8}$$

All these variables are normalized by the nominal inlet velocity, U_i. The most pronounced characteristic is the difference between $\bar{w}$ profiles. While there is almost no vertical velocity at the center of the jet for the two-sided baffle which deflects the jet both upward and downward, the downward velocity for the one-sided baffle is quite noticeable. Of course these are easily accounted for as due to the difference in the configuration of baffles. In the one-sided baffle case, the jet turns downward immediately after flowing out of the inlet, and this tendency is weak but present in the no baffle case also.

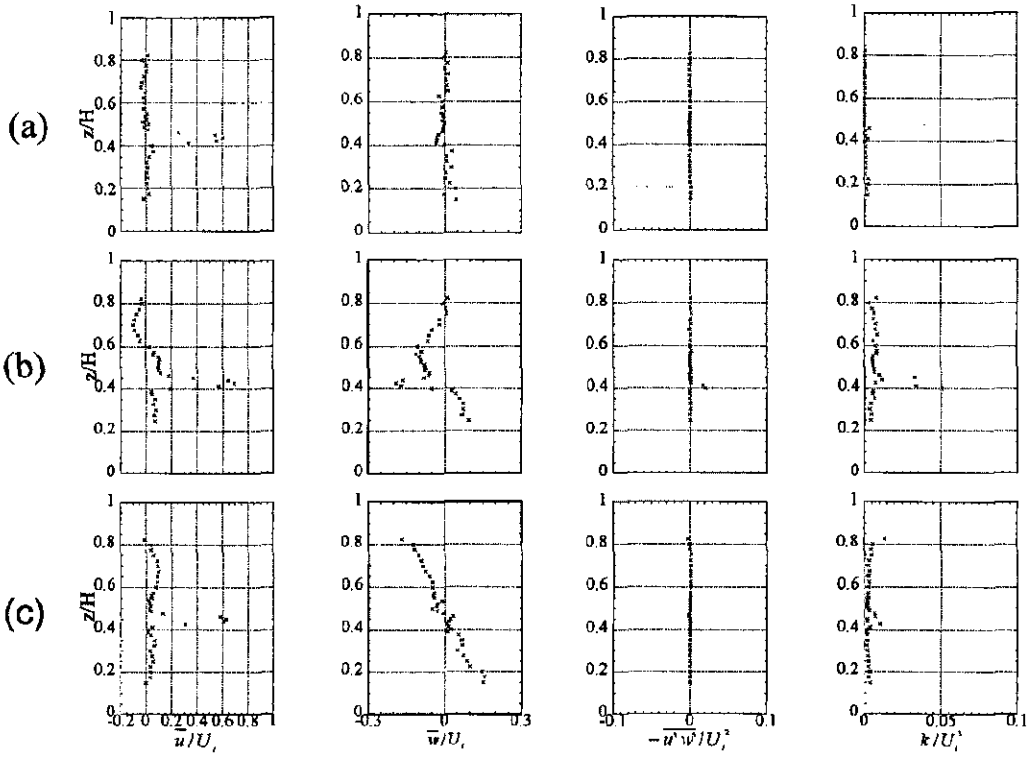

Fig. 3. Profiles of $\bar{u}/U_i$, $\bar{w}/U_i$, $-\overline{u'w'}/U_i^2$, and k/U_i^2 at x = 4 cm (x/H = 0.1)
(a) Case I; (b) Case II; (c) Case III

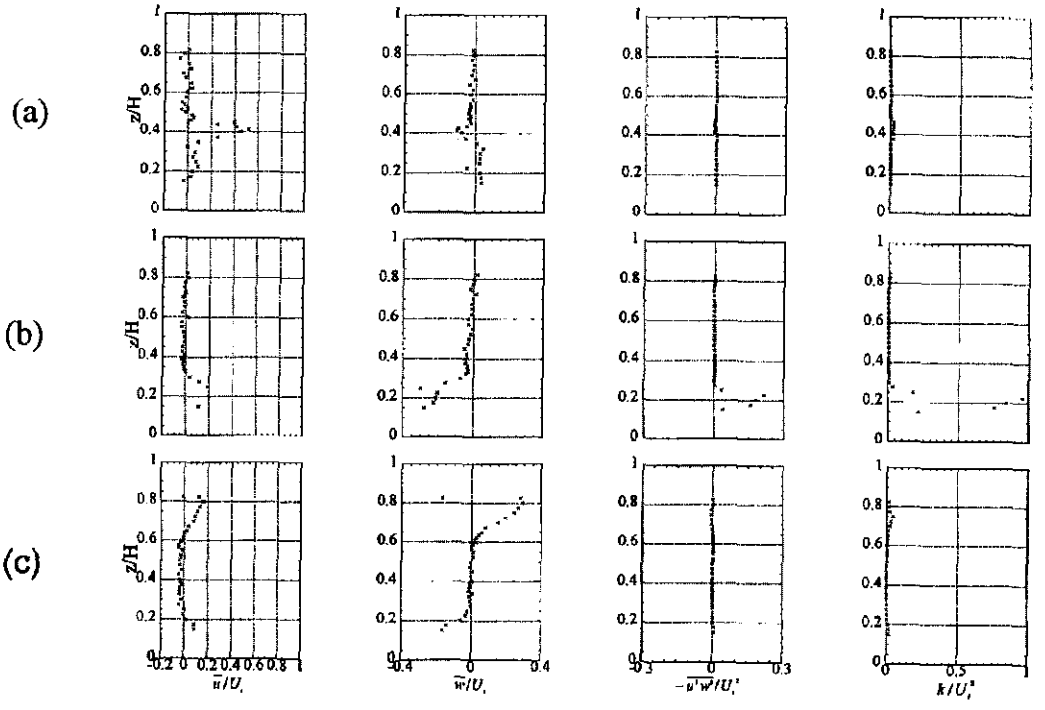

Fig. 4. Profiles of $\bar{u}/U_i$, $\bar{w}/U_i$, $-\overline{u'w'}/U_i^2$, and k/U_i^2 at x = 13 cm (x/H = 0.325)
(a) Case I; (b) Case II; (c) Case III

Consequently, a slightly downward inclination of the $\bar{u}$ profile is observed in the flow with the one-sided baffle. In the cases of both baffle types, $\bar{w}$ off the center of the jet shows upward velocity below the jet and downward velocity above the jet, from which it can be concluded that recirculation occurs in the region between the inlet and the baffle.

The spike in k and the $-\overline{u'w'}$ profile reflects the inlet shear layer bounding a potential-flow core. This spike is clearly seen in the one-sided baffle case, but not very clear in the cases of no baffle and two-sided baffle. Lyn and Rodi (1989) showed the same results and speculated that the vertical resolution of measuring was not fine enough and the shear layer itself was not fully turbulent. However their experiments and this experiment show the same results, that is, only one spike for the one-sided baffle case, and no spike or a not very pronounced spike for the two-sided baffle case. It seems too much to be coincidence. At this point no satisfactory explanation for the difference seems at hand.

Inspecting the $\bar{u}$ and $\bar{w}$ profiles in Fig. 4, which shows flow characteristics just downstream of the baffle, a large recirculation (negative $\bar{u}$) region is clearly noted. This region extends beyond the tips of the two-sided baffle both upward and downward. As Lyn and Rodi (1989) indicated, the large negative vertical velocities for both types of baffles would have the practical implication of the danger of erosion and resuspension of already settled particles. At the immediate downstream of baffles, the Reynolds shear stress and turbulent kinetic energy profiles have distinct spikes for the one-sided

baffle but not so for the two-sided baffle as at the immediate upstream of baffles, as is shown in Fig. 3.

To take a closer look at flow structures near the inlet, more detailed measurements were done for Cases I and III and are presented in Fig. 5 and Fig. 6. Velocity is nondimensonalized by nominal average velocity, U, for Cases I and III respectively, and Fig. 6 shows k distribution for the same cases. Measurements were done with the interval of 5 cm along the channel up to 50 cm *(x/H=1.25)* downstream except for x = 4 cm *(x/H=0.10)* and 13 cm *(x/H=0.325)*. The jet from the inlet without a baffle slides down and flows along the bottom with reverse flow being present above the jet flow as shown clearly in Fig. 5 (a). The jet with a two-sided baffle is deflected both upward and downward and reverse flow towards the baffle occupies the central region between two positive flows downstream as shown in Fig. 5 (b). The slot is located slightly lower than half the water depth (z/H = 0.475; z = 19 *cm*, H = 40 cm). If the relative slot position is higher, it is expected the jet flows rather toward the free surface, and this is verified by the experiment Case VI where the slot is located higher than half the water depth (z/H = 0.633; z = 19 cm, H = 30 cm). In these plots as well as in Fig. 6, the flows near the free surface and bottom are not present because of the limitation of the ADV and the instrument carriage .

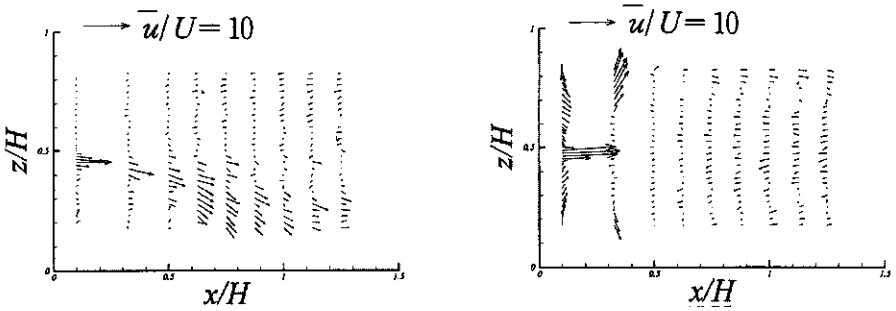

(a) Case I (b) Case III

Fig. 5. Velocity vector fields : (a) Case I ; (b) Case III

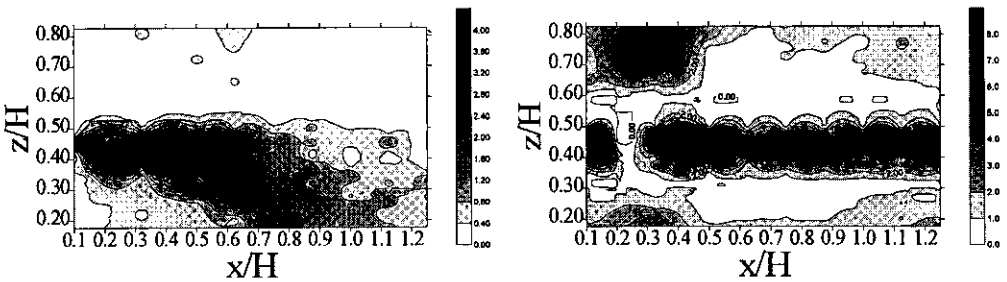

(a) Case I (b) Case III

Fig. 6. Contour of k/U^2 : (a) Case I ; (b) Case III

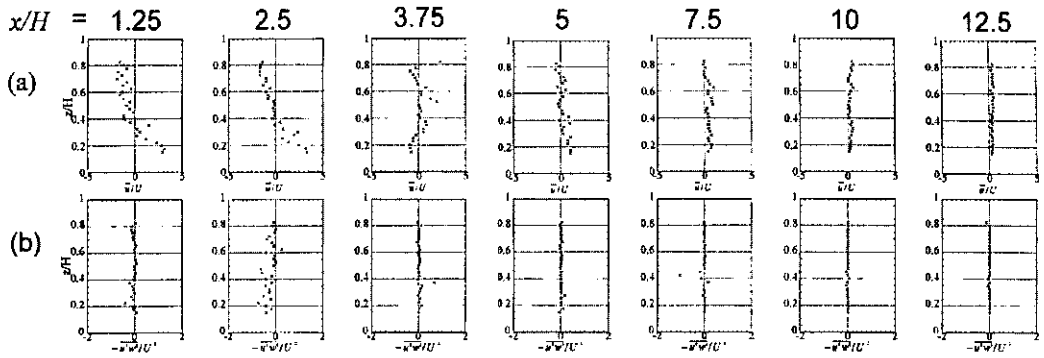

Fig. 7. Streamwise development of profiles for Case I at x/H = 1.25, 2.5, 3.75, 5, 7.5, 10, 12.5
(a) $\bar{u}/U$; (b) $-\overline{u'w'}/U^2$

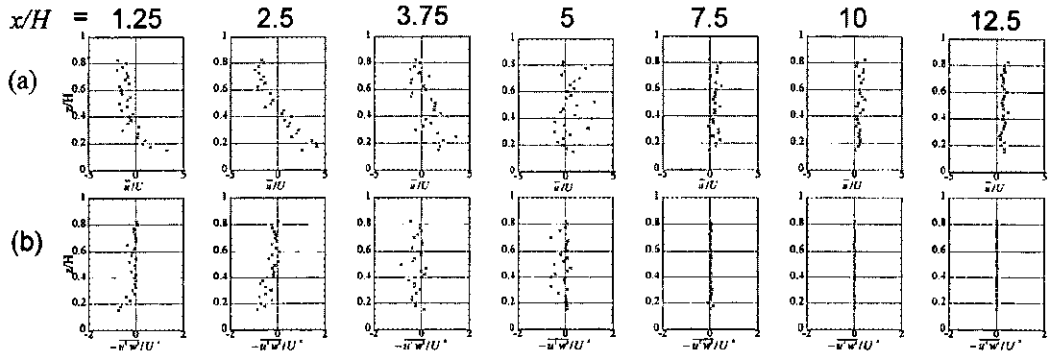

Fig. 8. Streamwise development of profiles for Case II at x/H = 1.25, 2.5, 3.75, 5, 7.5, 10, 12.5
(a) $\bar{u}/U$; (b) $-\overline{u'w'}/U^2$

Fig. 6 shows the contours of turbulent kinetic energy, k, nondimensionalized by U for Cases I and III. Since k is nondimensionalized by U, instead of U_i, unlike in Figs. 3 and 4, the variations of k look more pronounced near the inlet in Fig. 6 compared with those in Figs. 3 and 4. Between x = 13 cm and 50 cm, the maximum k appears to follow the central trajectory of the jet in the case of no baffle, and coincide with the parallel line with the height of the slot or is slightly lower than that in the case of the two-sided baffle. This line is approximately where the maximum reverse flow velocity occurs in the recirculation region.

The development of only $\bar{u}$ and $-\overline{u'w'}$ profiles among various profiles along the channel are presented in Fig. 7, 8, and 9 for Case I (no baffle), Case II (one-sided), and Case III (two-sided) respectively. In these profiles, nominal average velocity U, instead of U_i, is used for the nondimensionalization. The recirculation region deduced from the negative $\bar{u}$ is observed to extend to $x/H \approx 7.5$ for both Case I (no baffle) and Case II (one-sided), and $x/H \approx 5.0$ for Case III (two-sided baffle), but the vertical uniformity of $\bar{u}$ is achieved further downstream at $x/H \approx 10$ for all cases. Similar characteristics of nonuniformity in the profiles of the

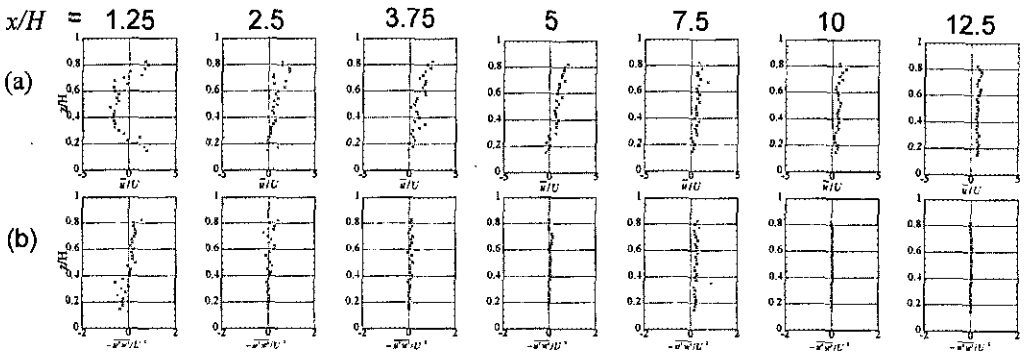

Fig. 9. Streamwise development of profiles for Case III at x/H = 1.25, 2.5, 3.75, 5, 7.5, 10, 12.5
(a) $\bar{u}/U$; (b) $-\overline{u'w'}/U^2$

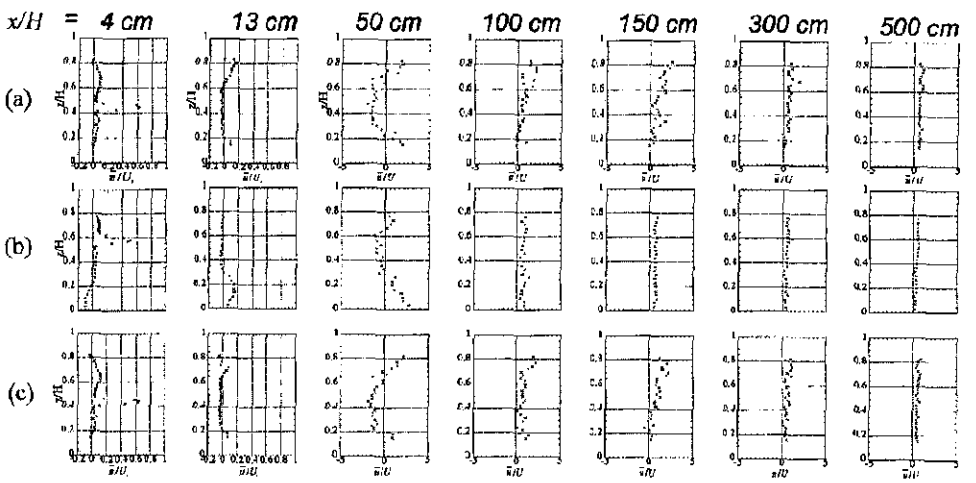

Fig. 10. Comparison of $\bar{u}/U_i$;($\bar{u}/U$ after x = 50 *cm*) profiles : (a) Case III; (b) Case V; (c) Case IX

Reynolds shear stress, $-\overline{u'w'}$, are observed in these figures.

Fig. 10 presents the comparison of the developments of the $\bar{u}/U_i$ ($\bar{u}/U$ where $x/H>1.25$) profiles for two-sided baffle cases with different discharge, Q, and depth, H. The profile (a) shows a strong vertical nonuniformity (higher velocity in the upper region) rather than approximate symmetry after the end of the recirculation region until it achieves uniformity far downstream, although the center of the slot is located slightly lower than half the water depth (z/H = 0.475). On the other hand, the case with higher relative slot height (z/H = 0.633) achieves the approximate uniformity immediately after the recirculation ends as shown in (b). Here it should be made clear that there are no velocity measurements near the free surface and in the reach between x/H =1.25 and 2.5. Besides, the profiles in (a) and (b) have different flow conditions as shown in Table 1. Therefore more experiments with different slot heights but with the same flow conditions are needed to draw a

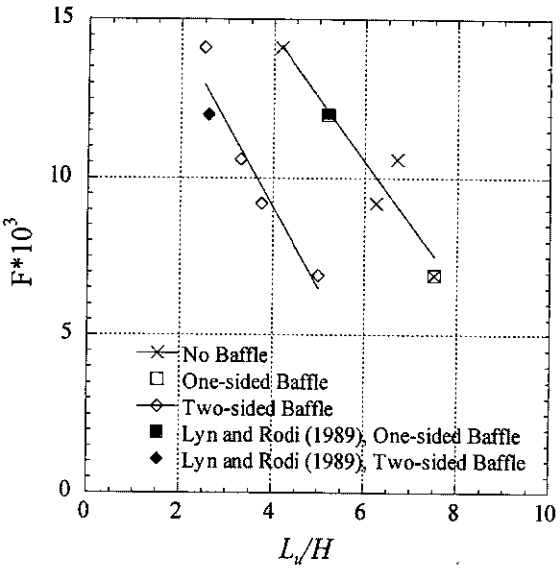

Fig. 11. Extent of Recirculation

definite conclusion about the role which the slot height plays.

Fig. 11 shows the effects of flow conditions and type of baffles on the extent of the recirculation region, L_u, based on the absence of reverse flow. Despite the lack of data, two general trends are clearly discernible. With the same **F**, the cases with the two-sided baffle clearly reduce the recirculation region compared with the cases with the one-sided baffle. Lyn and Rodi (1989) maintained that the double shear layers in the flow with the two-sided baffle promote more immediate vertical mixing. Also, it is clear that the higher **F** is, the shorter the inlet region for the same type of flows. Lumping one-sided baffle cases into no baffle cases, which can be justified in terms of the extent of the recirculation region as also indicated in Lyn and Rodi (1989), two linear regressional curves can be derived as follows.

$$\mathbf{F}^*10^3 = -2.58L_u/H + 19.4$$

two-sided baffle (9)

$$\mathbf{F}^*10^3 = -2.07L_u/H + 22.4$$

one-sided baffle and no baffle (10)

However, it should never be forgotten that the determination of the point where reverse flow ends is not as accurate as it is desired because the velocity profiles were measured every 50 cm along the channel after x = 50 *cm* and every 100 cm after x = 200 cm so that L_u/H could be in error by more than 1. It is obvious that achieving the ideal plug-flow is advantageous for the settling efficiency. However, it does not lead to the conclusion that a higher inlet velocity is desirable, because the overflow rate, *UH/L*, becomes larger so as to reduce solid removal efficiency. Although there might be a compromise between these two factors it cannot be clarified until further research is performed incorporating solid removal processes.

4. CONCLUSIONS

A series of laboratory experiments of neutrally buoyant two-dimensional jet impinging on two types of baffles and without a baffle was carried out to obtain velocity and turbulence data. Results of the velocity measurements show that recirculation occurs in the region between the inlet and the baffle for the cases of both baffle types. A large recirculation also occurs downstream of the baffle. This recirculation region extends to $x/H \approx 7.5$ for cases of the one-sided baffle and the no baffle, whereas it extends to $x/H \approx 5.0$ for the case of the two-sided baffle.

The use of the two-sided baffle resulted in the shortest inlet region and the fastest establishment of plug-flow approximation due to the double shear layers. In addition to the type of the baffle, the Froude number turned out to be an important factor in the extent of the inlet region. The higher **F** was, the shorter the inlet region.

ACKNOWLEDGEMENTS

This research work was partially supported by the 1999-2000 Research Fund 1999-2-309-004-3 of the Korea Science and Engineering Foundation and the 1999-2000 Brain Korea. The general support provided by the Research Institute of Engineering Science of Seoul National University, Seoul, Korea are also appreciated.

REFERENCES

Anderson, N. E. (1945). "Design of settling tanks for activated sludge." *Sewage Works Journal*, Vol. 17, No. 1, pp. 50-63.

Hazen, A. (1904). "On sedimentation, Transactions." ASCE, Vol. 53, pp. 45-71.

Krebs, P., Vischer, D. and Gujer, W. (1995). "Inlet-Structure design for final clarifiers." *Journal of Environmental Engineering*, ASCE, Vol. 121, No. 8, pp. 558-564.

Krebs, P., Armbruster, M. and Rodi W. (1998). "Laboratory experiments of buoyancy- influenced flow in clarifiers." *Journal of Hydraulic Research*, Vol. 36, No. 5, pp. 831-851.

Lyn, D. A. and Rodi, W. (1989). "Turbulence measurement in model settling tank." *Journal of Hydraulic Engineering*, ASCE Vol. 116, No. 1, pp. 3-21.

Raju, K. G. R., Kothyari, U. C. and Saxena, M. (1999). "Sediment removal efficiency of settling basins." *Journal of Irrigation and Drainage Engineering*, ASCE Vol. 125, No. 5, pp. 308-314.

Younghan Kim, Grad. Student, Department of Civil Engineering, Seoul National University, San 56-1, Sinlim-Dong, Gwanak-Gu, Seoul 151-742, Korea.
(E-mail: yhkim@gong.snu.ac.kr)

Il Won Seo, Assoc. Prof., Department of Civil Engineering, Seoul National University, San 56-1, Sinlim-Dong, Gwanak-Gu, Seoul 151-742, Korea.
(E-mail: seoilwon@plaza.snu.ac.kr)

Jungkyu Ahn, Grad. Student, Department of Civil Engineering, Seoul National University, San 56-1, Sinlim-Dong, Gwanak-Gu, Seoul 151-742, Korea.
(E-mail: ajk38317@orgio.net)

(Received August 17, 2000, accepted January 4, 2001)